Reactive and Functional Polymers 112 (2017) 74–80

Contents lists available at ScienceDirect

Reactive and Functional Polymers

journal homepage: www.elsevier.com/locate/react

Fabrication and gas sensing behavior of poly(3,4-ethylenedioxythiophene) coated polypropylene fiber with engineered interface

Xingping Wang [a], Si Meng [a], Wujun Ma [a], Jürgen Pionteck [b], Minoj Gnanaseelan [b], Zhe Zhou [a], Bin Sun [a,*], Zongyi Qin [a], Meifang Zhu [a,*]

[a] State Key Laboratory for Modification of Chemical Fibers and Polymer Materials, College of Materials Science & Engineering, Donghua University, 2999 North Renmin Road, Shanghai 201620, China

[b] Leibniz Institute of Polymer Research Dresden, Hohe Straße 6, 01069 Dresden, Germany

ARTICLE INFO

Article history:
Received 2 November 2016
Received in revised form 16 January 2017
Accepted 19 January 2017
Available online 20 January 2017

Keywords:
Poly(3,4-ethylenedioxythiophene)
Conductive composite fiber
Gas sensing
Surface modification
Photoinduced surface grafting

ABSTRACT

Conductive composite fibers were successfully fabricated by coating poly(3,4-ethylenedioxythiophene) (PEDOT) layers on the surface of polypropylene-graft-poly(acrylic acid) (PP-g-PAA) fibers through *in situ* chemical oxidative polymerization. It was found that the adhesion between the conductive PEDOT layers and the modified PP fiber substrates was significantly enhanced due to the electrostatic attractions between PEDOT chains and carboxylic groups of grafted PAA. In this study, we investigated the influence of the 3,4-ethylenedioxythiophene (EDOT) concentration and the oxidant species on the electrical conductivity of the composite fibers, and the result show that the maximum conductivities of PP-g-PAA/PEDOT composite fibers prepared with $FeCl_3$ and iron(III) p-toluenesulfonate (FepTS) as oxidants reached 0.069 S/cm and 10.09 S/cm, respectively. The composite fibers were applied as a sensor for HCl and NH_3 gas detection and exhibited a rapid and reversible response. The influence of the oxidant species on the sensing properties for HCl and NH_3 gas detection is further discussed, and some features such as fast response time (less than 2 s) and high relative resistance changes (63% for HCl and 110% for NH_3 gas) were achieved.

1. Introduction

Smart materials like piezoelectric materials [1], shape-memory materials [2], self-healing materials [3], sensors [4], *etc.*, have flourished rapidly in this decade. Commercial smart materials are based on ceramics or metal alloys which require high temperature and robust processing conditions and machineries. To achieve a degree of commercial success facile conditions and process to prepare smart materials which could be integrated with continuous mass production is indispensable. Smart textiles are those materials where the smart component is backed up by the textile which bestows flexibility, easy fabricability, mass productivity and integrability.

Intrinsically conducting polymers (ICPs) are primarily used for supercapacitors [5], electrochromic devices [6], photovoltaic devices [7], and sensors [8–12]. However, the applications of these ICPs have been limited by their complex production process and the poor mechanical flexibility resulting from their rigid conjugated backbone structure. Almost in all applications, conducting polymers are backed up by a substrate either plastic or ceramic owing to its poor mechanical strength [13]. To address these drawbacks, ICPs were also used to form electrically conductive composite fibers with various insulating fibers by *in situ* polymerization [14,15]. Owing to the advantages of the excellent flexibility of the substrate and the electrical conductivity, the electrically conductive composite fibers as flexible smart materials are used in various fields such as heat generators [16], electromagnetic interference shielding [17], strain sensors [18] and flexible or stretchable conductors [19]. In this work, we take the advantage of its reversible redox ability to fabricate and characterize smart textile sensor. ICPs coated fabric is a promising medium for chemical sensing of analytes that are electronically active when encountering the conducting polymers at room temperature, which can cause changes in resistance of the sensing materials [20]. Recently, polyaniline coated fabrics [21–23] and polypyrrole coated fabrics [24] have been utilized as sensing materials to detect pH and various hazardous gas such as ammonia, nitrogen dioxide, carbon monoxide, and propane. Among a wide variety of ICPs, PEDOT is now regarded as one of the most promising conducting polymers for practical applications on account of its high conductivity, good processability, excellent thermal and chemical stability [25].

* Corresponding authors.
E-mail addresses: sunbin@dhu.edu.cn (B. Sun), zhumf@dhu.edu.cn (M. Zhu).

http://dx.doi.org/10.1016/j.reactfunctpolym.2017.01.007
1381-5148/

However, fabrication of conductive composite fibers based on ICPs suffer from the limitation of the poor adhesion between the conductive coating and the synthetic fiber substrates due to the low surface energy of most conventional polymeric materials. To overcome these problems, effective strategies are required to improve the adhesion between the ICPs and the polymeric substrates. Although *in situ* polymerization or oxidative chemical vapor deposition of PEDOT on nylon 6, PET fabric, and viscose fabric are recently reported [26,27], little research has been explored to improve the adhesion between the PEDOT coating and the polymeric substrates and to develop sensors based on PEDOT coated fabrics.

Herein, we fabricated a flexible composite fiber based on PEDOT as sensor for HCl and NH_3 gas. Electrically conducting layers of PEDOT were tightly coated onto the surface of PP-g-PAA fiber substrate *via in situ* polymerization (illustrated in Scheme 1). Moreover, the performance of the as-prepared PP-g-PAA/PEDOT composite fibers as chemical sensors for detecting HCl and NH_3 gas was evaluated and the sensing mechanism was discussed.

2. Experimental

2.1. Materials

Commercial multifilament PP fibers (monofilament with a diameter of 33 μm) were extracted by acetone for about 24 h to remove additives before use. Acrylic acid (AA), benzophenone (BP), acetone, ethanol, and $FeCl_3$ were obtained from Sinopharm Chemical Reagent Co. Ltd., China. EDOT monomer and FepTS were purchased from Energy-Chemical Co. Ltd., China. All reagents were of analytical grade and used without any further purification.

2.2. Preparation of PP-g-PAA/PEDOT composite fibers

2.2.1. Photo-induced graft polymerization of AA from PP fiber surfaces

Ma et al. [28] developed a sequential two-step photo-induced living graft polymerization process to decrease unwanted homo-polymerization and graft surface-confined polymer layers, where radical sites were first formed under UV irradiation with a photo-initiator molecule, and then monomers polymerize from these reactive sites. A similar procedure was followed to obtain PP-g-PAA fibers reported here.

A total number of 20 PP fibers were fixed onto a 12 × 1 cm rectangular copper frame using stainless steel clips, and then dip-coated in a 5 vol.% solution of BP in ethanol for 10 min. The specimen was removed from the solution and dried at room temperature for 30 min to evaporate the ethanol. The specimen was then carefully transferred into a quartz test tube and purged with nitrogen. UV irradiation of the fibers was performed for 10 min by a LED-UV processor (UVATA-UPA100 series; UVATA Precision Optoelectronics CO., LTD). The processor has a wavelength of 365 ± 5 nm and an intensity of 450 mW/cm^2 when the distance between UV lamp and fiber surface was 50 mm. After irradiation, the substrate was taken out of the quartz test tube, sonicated in ethanol for 10 min to remove any unreacted BP, and then dried at room temperature.

The BP grafted PP fibers were then immersed into 40 mL AA/water solution with different concentrations, the dissolved oxygen in the reaction solution was removed by bubbling nitrogen for 60 min at flow rate of 5 L/min, and then exposed to the UV irradiation (450 mW/cm^2 at 365 nm) for a specified time. After irradiation, the substrate was sonicated in water for 30 min to remove any unreacted acrylic acid. The non-grafted PAA was removed by soaking the fibers in deionized water for 2 h at 100 °C. Finally, the fibers were dried under vacuum for 24 h for further use.

2.2.2. In situ polymerization of PEDOT onto the PP-g-PAA fiber surfaces

According to literature [29], the oxidative *in situ* polymerization is best carried out with ionic oxidants in a suitable higher oxidation state like iron-III. Normally, to obtain the PEDOT with the high conductivity, the optimum mole ratio of iron-III and EDOT monomer is 2.3:1. Therefore, this mole ratio was also used in this work. The PP-g-PAA fibers were immersed in 5 mL ethanol solution of EDOT and oxidant with varying concentration for 30 min. During this period, the solution was maintained at about 0–5 °C for inhibiting the polymerization during immersion. After that, the PP-g-PAA fibers were removed from the reaction solution and dried under atmospheric conditions (25 °C, relative humidity 60%) for 24 h. EDOT on the surface of the PP-g-PAA fibers polymerized to PEDOT during this drying process. A control specimen was prepared following the same procedure using the neat PP fibers as substrate. The as-prepared PP-g-PAA/PEDOT composite fibers were subsequently rinsed with deionized water and ethanol under ultrasonic treatment for up to 1 h to remove the residual reactants and oligomer, and then dried in vacuum at 40 °C for 24 h.

In this paper, EDOT were polymerized on the surface of PP-g-PAA fibers either with FepTS or $FeCl_3$, thus the composite fibers were denoted as PP-g-PAA/PEDOT-FepTS and PP-g-PAA/PEDOT-$FeCl_3$, respectively.

2.3. Characterization

The surface morphologies of pristine PP fibers and as-prepared composite fibers were observed using a JEOL JSM-5600LV.

The chemical structures of pristine PP fibers and as-prepared composite fibers were characterized by attenuated total reflectance Fourier transform infrared (ATR-FTIR) Spectroscopy. ATR-FTIR spectra were recorded on Nicolet 6700 with variable angle horizontal ATR accessory, on which a 45° rectangle ZnSe crystal was used. The intensities of characteristic peak at wavenumber 1705 cm^{-1}, corresponding to the —C═O stretches in the carboxylic acid groups of PAA, and the peak at wavenumber 1376 cm^{-1}, corresponding to the CH_2 and CH_3 groups of PP were used for analysis. Results are presented as peak area ratio

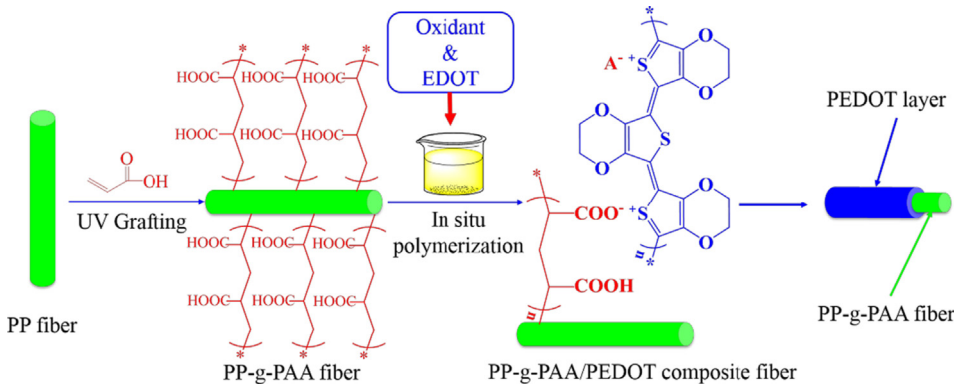

Scheme 1. Illustration of the fabrication mechanism of the PP-g-PAA/PEDOT composite fibers (where A^- is the dopant anion: chloride or p-toluenesulfonate).

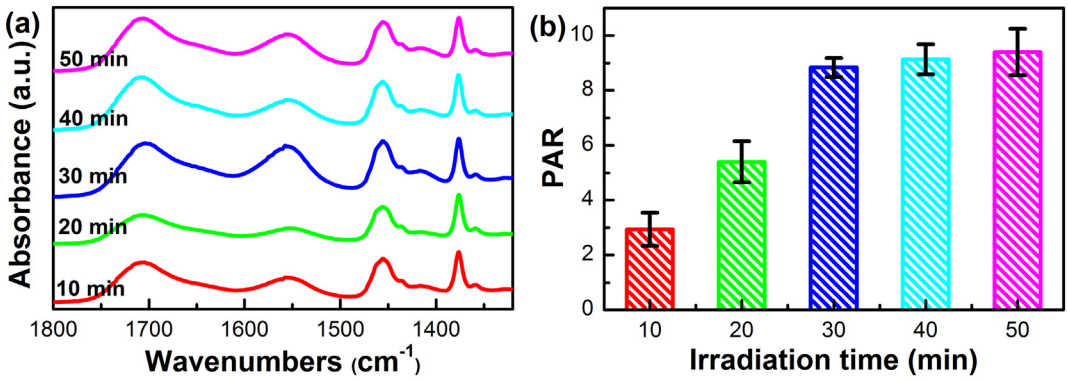

Fig. 1. (a) ATR-FTIR spectra and (b) PAR of PP-g-PAA fibers reacted in 20 vol.% AA solution with different irradiation times.

(PAR), *e.g.*, peak area at 1705 cm^{-1} divided by the peak area at 1376 cm^{-1}.

The electrical resistance of PP-g-PAA/PEDOT composite fiber was measured by two point probe method, in which probes were connected to a Keithley 2000 source meter. The electrical conductivities of the composite fibers were calculated using the following equation:

$$\sigma = \frac{L}{R \times S} \tag{1}$$

where σ is the electrical conductivity (S/cm), R is the electrical resistance (Ω), and L and S are the length (cm) and cross section area (cm^2) of the composite fibers, respectively.

The thermogravimetric analysis (TGA) was performed on a TA Q5000IR thermogravimetric analyzer with programmed heating at 10 °C/min from 50 °C to 600 °C. The chamber was continuously swept with N_2 at 20 mL/min.

2.4. Gas sensing test

The conductive PP-g-PAA/PEDOT composite fibers were initially exposed to NH_3 (g) and HCl (g) to evaluate their sensing properties to toxic gases which could interact electronically with conductive PEDOT layer. The gas sensing properties of PP-g-PAA/PEDOT composite fibers were investigated by recording their resistance change upon alternate exposure to 1% NH_3 gas (or 1% HCl gas) for 120 s and dry air for 180 s at 20 °C. A homemade testing device (according to [30]) connected to a digital multimeter (Keithley 2000, USA) was used in this research to monitor the variation of electrical resistance. The resistance measurement set-up was interfaced with a computer to record the real-time resistance of the composite fiber upon exposure to analytes. To compare the sensing properties of composite fibers polymerized with different oxidants independently of their initial electrical resistance, the normalized resistance changes R_{REL} were calculated according to Eq. (2),

$$R_{REL}(\%) = \left(\frac{R - R_I}{R_I}\right) \times 100 \tag{2}$$

where R_I is the initial resistance of the sample in the dry air and R is the real-time resistance upon exposure to 1% NH_3 gas (or 1% HCl gas).

3. Results and Discussion

3.1. Photo-induced graft polymerization of AA from PP fiber surfaces

The influence of graft polymerization reaction conditions on PAR was investigated. The ATR-FTIR spectra and PAR of PP fibers modified by photo-grafting with AA at different irradiation time in 20 vol.% acrylic acid solution in water are shown in Fig. 1. As expected, the amount of grafted PAA on PP fibers increases with increasing UV irradiation time, and this may be attributed to the formation of more active radicals on the fiber surface. However, no significant increase in the PAR was observed for UV irradiation times longer than 30 min. This result indicates that the amount of grafted PAA can be controlled by UV irradiation time. In addition, the dependence of PRA on monomer concentration was also investigated (Fig. 2(b)).

Fig. 2 shows the ATR-FTIR spectra and PAR of PP fibers modified by photo-grafting with AA at different concentration at the irradiation time of 30 min. The amount of grafted PAA also significantly increases with increasing AA concentration in the solution. The results indicate that the grafting efficiency of PAA on the surface of PP fiber could be controlled effectively by adjusting UV irradiation time and AA concentration. However, with increasing AA concentration at the irradiation time of 30 min, the solution changed from a clear solution to a soft

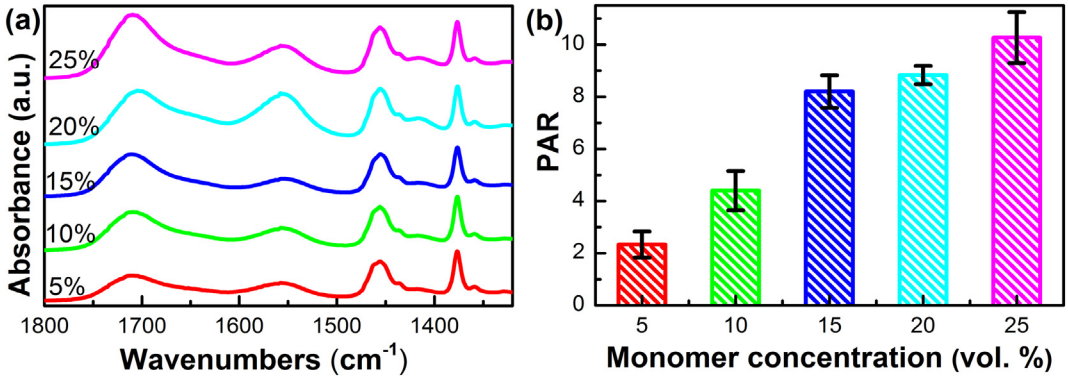

Fig. 2. (a) ATR-FTIR spectra and (b) PAR of PP-g-PAA fibers reacted in different AA concentration solution with 30 min UV irradiation.

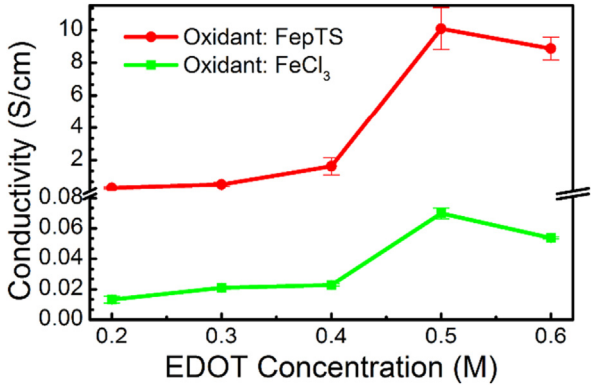

Fig. 3. Effect of the oxidant concentration on the conductivity of (a) PP-g-PAA/PEDOT-$FeCl_3$ composite fibers and (b) PP-g-PAA/PEDOT-FepTS composite fibers; impregnation temperature/time = 0–5 °C/30 min; polymerization temperature/time = 25 °C/24 h; mole ratio of oxidant to EDOT monomer = 2.3/1.

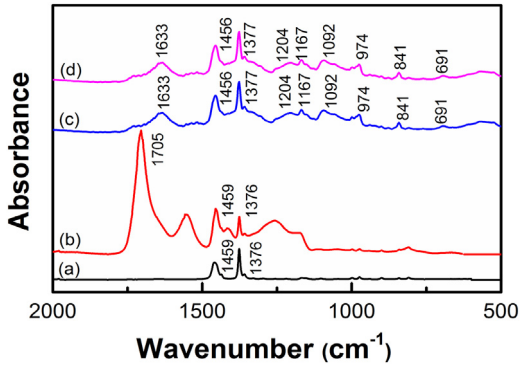

Fig. 5. ATR-FTIR spectra of (a) neat PP fibers, (b) PP-g-PAA fibers (irradiation time = 30 min; AA concentration = 20 vol.%; UV irradiation intensity = 450 mW/cm^2), (c) PP-g-PAA/PEDOT-$FeCl_3$ composite fibers and (d) PP-g-PAA/PEDOT-FepTS composite fibers.

gel, then to a firm gel due to the formation of ungrafted homopolymer in the solution. The 25 vol.% AA solution became a firm gel after 30 min reaction, and it is difficult to remove the fibers from the solution. Therefore, all the PP-g-PAA fibers used in the subsequent experiments were prepared at an irradiation time of 30 min in 20 vol.% acrylic acid solution.

3.2. Chemical structure of PP and composite fibers

The ATR-FTIR spectra of pristine PP fibers, PP-g-PAA fibers, and PP-g-PAA/PEDOT composite fibers are shown in Fig. 5. Fig. 5(a) represents a typical IR spectrum of pristine PP fibers (with a strong absorption of C—H deformation vibration at 1459 and 1376 cm^{-1}). The peak at 1376 cm^{-1} corresponding to the CH2 and CH3 groups of PP can be observed in all these spectra [31]. The ATR-FTIR spectra of PP-g-PAA fiber is shown in Fig. 5(b). The vibrations at 1705 cm^{-1} can be assigned to the C═O stretching, which is due to the carboxylic group in PP-g-PAA fiber [32]. The spectra for PP-g-PAA/PEDOT-$FeCl_3$ composite fiber (Fig. 5(c)) and PP-g-PAA/PEDOT-FepTS composite fiber (Fig. 5(d)) show a similar pattern and peak positions. Some characteristic broad bands of PEDOT are observed. The peaks at 1633 and 1377 cm^{-1} correspond to the C═C and C—C stretching of the quinoidal structure of the thiophene ring; the bands around 1204, 1167, and 1092 cm^{-1} are ascribed to vibration modes of ethylenedioxy group [19]. Further vibrations from C—S bond in the thiophene ring can be seen at 974, 841, and 691 cm^{-1} [33]. The ATR-FTIR results indicate that PEDOT was successfully deposited on the PP-g-PAA fiber.

3.3. Morphologies of PP and composite fibers

SEM was employed to examine the surface morphology of the PP-g-PAA fibers and the PP-g-PAA/PEDOT composite fibers. The pristine PP fiber with a diameter of 33 μm (Fig. 4(a)) has a smooth surface while the PP-g-PAA fiber (Fig. 4(b)) has a rough surface with a mean diameter of 37 μm, implying the thickness of the PAA layer to be around 2 μm. This increase in the diameter size correlates with the ATR-FTIR results proving the presence of thin surface coverage of PAA. Fig. 4(c) shows the SEM picture of a PP-g-PAA/PEDOT-FepTS composite fiber after 60 min sonicating in water. A dense and uniform layer of PEDOT particles was formed on the PP-g-PAA fiber surface. The PEDOT coating prepared by use of $FeCl_3$ exhibits rough structure as in case of use FepTS and is not shown here. For comparison, the pristine PP fiber was used as substrate to prepare PP/PEDOT composite fiber. The SEM picture of this PP/PEDOT composite fiber after 60 min washing under ultrasonic treatment is presented in Fig. 4(d). After washing, the diameter of PP/PEDOT composite fiber return to 33 μm, the deposited PEDOT particles were nearly completely washed away, and only few remaining PEDOT particles were observed, thus the fibers lose their conductivity. This may be attributed to the poor adhesion between PEDOT and pristine PP fiber. The low surface free energy and hydrophobic surface of pristine PP fiber were passive to adhesion. This demonstrated that grafting of PAA on PP fiber significantly improves the adhesion of PEDOT with the PP fiber substrate due to the electrostatic forces between PEDOT chains and carboxylic groups.

3.4. Thermal stability of PP and composite fibers

TGA was performed on PP and composite fibers in order to assess the relative thermal stability and the amount of PEDOT coatings on the fibers. The TGA curves of pristine PP fibers, PP-g-PAA fibers, PEDOT particles, and PP-g-PAA/PEDOT composite fibers prepared with different oxidants, $FeCl_3$ and FepTS are shown in Fig. 6. No observable weight loss or decomposition was observed at temperatures up to 400 °C for the pristine PP fibers, indicating excellent thermal stability. For PP-g-PAA fibers, the weight loss started at about 200 °C and nearly 80 wt% was lost by 460 °C, and about 96 wt% was lost by 600 °C. The chemical modification has a slight destabilizing effect on the PP fiber matrix. The TGA curves obtained with PEDOT exhibited weight losses around 150 °C and 300 °C. The small mass loss of about 10 wt% between 150 and 200 °C corresponds to the vaporization of adsorbed water and the loss of residual oligomers in the polymers [7]. The weight loss at

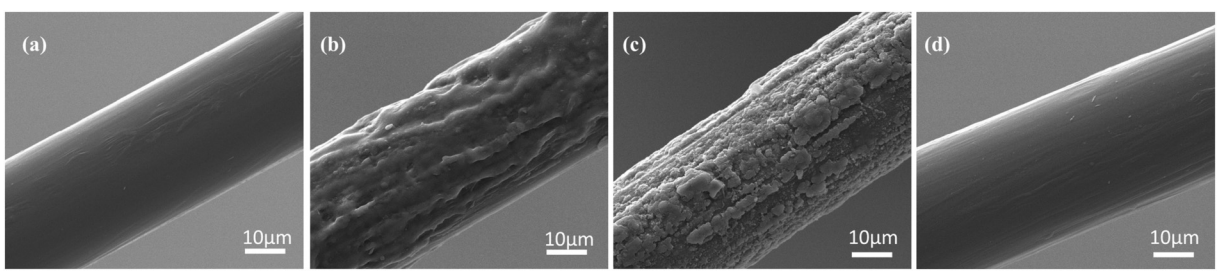

Fig. 4. SEM photographs of (a) pristine PP fiber, (b) PP-g-PAA composite fiber, (c) PP-g-PAA/PEDOT-FepTS composite fiber, and (d) PP/PEDOT composite fiber.

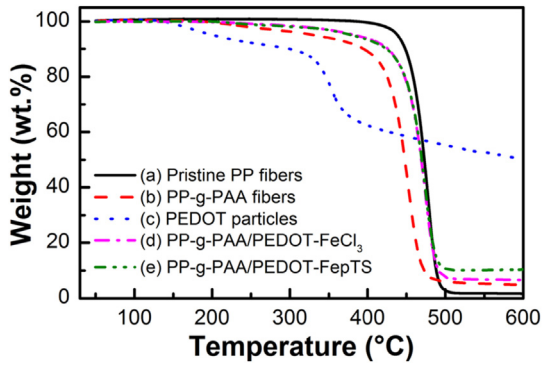

Fig. 6. TGA curves of (a) pristine PP fibers, (b) PP-g-PAA fibers, (c) PEDOT particles (oxidant (FepTS) concentration = 1.15 M; EDOT concentration = 0.5 M), (d) PP-g-PAA/PEDOT-$FeCl_3$ composite fibers, and (e) PP-g-PAA/PEDOT-FepTS composite fibers.

temperatures above 300 °C may be attributed to the degradation and decomposition of the PEDOT main chains [34]. The PEDOT shows a residual amount of 50.2 wt% after heating to 600 °C. The TGA curves of PP-g-PAA/PEDOT composite fibers polymerized with different oxidants $FeCl_3$ (Fig. 6(d)) and FepTS (Fig. 6(e)) displayed similar pattern, nearly overlapping in degradation curve, except with higher residual at the end for PP-g-PAA/PEDOT-FepTS composite fiber. The weight loss of PP-g-PAA/PEDOT composite fibers started at about 200 °C, and this can attribute to the loss of residual oligomers in PEDOT and the loss of PAA coating. The major decomposition occurs in the region between 300 and 500 °C due to the decomposition of the PEDOT, PP-g-PAA, and the PP main chains. Assuming that there is an additive degradation behavior of the PP-g-PAA/PEDOT sample, and taking the residuals of the PEDOT, PP-g-PAA fibers, PP-g-PAA/PEDOT-$FeCl_3$ composite fibers, and PP-g-PAA/PEDOT-FepTS composite fibers at 600 °C (50.2, 4.8, 6.6 and 10.4 wt%, respectively), one can estimate the PEDOT content in PP-g-PAA/PEDOT-$FeCl_3$ composite fibers and PP-g-PAA/PEDOT-FepTS composite fibers to be 3.9 and 12.3 wt%, respectively. It assumed that besides of the higher viscosity of the FepTS/ethanol solution compared to $FeCl_3$/ethanol solution, the polymerization efficiency in the former case is better than in the latter case. Therefore, there were more PEDOT coated on the PP-g-PAA fibers when FepTS was employed as oxidant.

3.5. Conductivities of PP-g-PAA/PEDOT composite fibers

The PP-g-PAA composite fibers were used as substrate for *in situ* polymerization of EDOT. Fig. 3 shows the relationship between the electrical conductivity of PP-g-PAA/PEDOT composite fibers and the EDOT concentrations with different oxidants.

Due to the very rough structures of the PAA coating and the final PEDOT coating, the effective resistance of the conductive coating layer could not be determined. Thus, for calculation σ, the overall diameter of the coated fibers estimated from the SEM analysis was used. The conductivity of PP-g-PAA/PEDOT composite fibers underwent an initially significant increase, and reached a maximum value at the concentration of 0.5 M. With further increase in EDOT concentration, the conductivities finally presented a downward trend. This may be because of the formation of large amount of PEDOT particles in the mixture solution rather than on the surface on the PP-g-PAA fibers at a higher EDOT concentration. Therefore, it was concluded that the optimum concentration of EDOT monomer and oxidant are 0.5 M and 1.15 M, respectively. The conductivities of the PP-g-PAA/PEDOT-$FeCl_3$ and PP-g-PAA/PEDOT-FepTS composite fibers ranged from 0.013 S/cm to 0.069 S/cm and 0.29 S/cm to 10.09 S/cm, respectively. Overall, the conductivities of PP-g-PAA/PEDOT-FepTS composite fibers were about 2 orders of magnitude higher than those of PP-g-PAA/PEDOT-$FeCl_3$ composite fibers. This cannot be attributed just to the higher grafting degree in case of FepTS (see TGA result) but mainly by the higher doping level of PEDOT when polymerized with FepTS rather than with $FeCl_3$ because the electronegativity of FepTS is stronger than that of $FeCl_3$ [26]. Moreover, $FeCl_3$ is not suitable for preparing high conductivity PEDOT due to the formation of unwanted non-conductive neutral PEDOT [29]. Therefore, all the PP-g-PAA/PEDOT composite fibers used in the subsequent characterization were prepared at the optimum polymerization condition: impregnation temperature/time = 0–5 °C/30 min; polymerization temperature/time = 25 °C/24 h; oxidant concentration = 1.15 M; EDOT concentration = 0.5 M.

3.6. Acid-base gas sensing behaviors of PP-g-PAA/PEDOT composite fibers

In order to achieve stable resistance responses, the fibers prepared at the optimum polymerization conditions (impregnation temperature/time = 0–5 °C/30 min; polymerization temperature/time = 25 °C/24 h; oxidant concentration = 1.15 M; EDOT concentration = 0.5 M) with different oxidants were selected for gas sensing investigations.

Fig. 7(a) shows the reversible and reproducible response of PP-g-PAA/PEDOT-FepTS and PP-g-PAA/PEDOT-$FeCl_3$ composite fibers upon periodic exposure to HCl/air (120 s/180 s) at 20 °C. In the first cycle, the electrical resistances of the composite fibers decreased immediately after exposure to 1% HCl gas and 50% of the resistance change happened during the first 5 s of exposure to HCl. Upon exposure to HCl gas, HCl molecules diffuses into the PEDOT layer, Cl^- gets incorporated into the PEDOT backbone as an additional dopant anion, which leads to the increase in the doping level, thereby enhancing the electric conductance of PEDOT due to an increase in the number of charge carriers [12,35]. The speculated sensing mechanism is illustrated in Fig. 7(b). After the HCl gas flow was replaced by dry air flow, the resistance of the composite fiber increased quickly. However, the resistance of the composite fiber could not be recovered to the initial level. This may be attributed to the residual HCl molecules in the PEDOT backbone which causes permanent enhancement of electrical conductance.

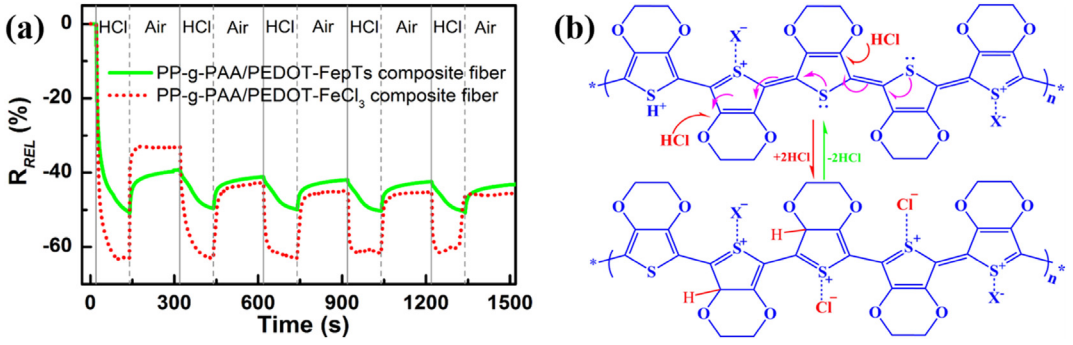

Fig. 7. The reversible and reproducible response of PP-g-PAA/PEDOT composite fibers upon periodic exposure to HCl (1%)/air (a) and the possible reaction mechanism in the HCl gas sensing process (b).

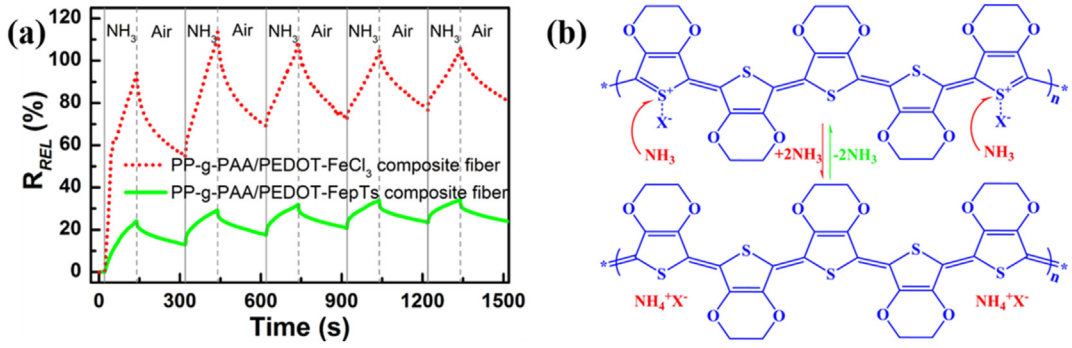

Fig. 8. The reversible and reproducible response of PP-g-PAA/PEDOT composite fibers upon periodic exposure to NH_3 (1%)/air (a) and the possible reaction mechanism in the NH_3 gas sensing process (b).

Fig. 8(a) shows the reversible response of PP-g-PAA/PEDOT-FepTS and PP-g-PAA/PEDOT-$FeCl_3$ composite fibers upon periodic exposure to NH_3 and dry air (120 s/180 s) at 20 °C. The electrical resistance of the composite fibers increased immediately after they were exposed to 1% NH_3 gas. The diffusion of NH_3 into PEDOT layer dedopes the conducting polymer, eventually leading towards the formation of a neutral PEDOT backbone resulting in a decrease in number of charge carriers (illustrated in Fig. 8(b)), which causes a significant drop in conductivity. In addition, the $NH_4^+X^-$ decomposed back into ammonia when exposed to air, which caused the recovery of conductivity. Yet, the electrical resistance of the composite fibers could not recover completely due to the residual NH_4^+ ions in the PEDOT backbone which inflicts the irreversible change of conductance. As in the case of HCl sensing, starting from the second cycle the response is rather stable.

As can be seen from Fig. 7(a) and Fig. 8(a), the response of PP-g-PAA/PEDOT-$FeCl_3$ composite fibers to HCl and NH_3 gas is faster and stronger than that of PP-g-PAA/PEDOT-FepTS composite fibers. The result suggests that a bigger change in resistance is associated with lower doping degree of PEDOT due to the different oxidants which also functions as dopant used in the polymerization.

4. Conclusions

PP-g-PAA/PEDOT conductive composite fibers could be prepared through *in situ* chemical polymerization of EDOT monomers on the surface of functionalized PP fibers. The conductive fibers exhibited the combination of flexibility of PP fiber, excellent conductivity of PEDOT, and especially structural stability benefited from the strong electrostatic attractions between PEDOT and carboxylic groups of grafted PAA. EDOT concentrations and oxidant species effect the degree of EDOT grafting and reachable conductivities. The maximum conductivities of PP-g-PAA/PEDOT composite fibers polymerized with oxidant $FeCl_3$ and FepTS reached 0.069 S/cm and 10.09 S/cm, respectively. The oxidant species has a significant impact on the sensing performance for HCl and NH_3 gas. This is due to the different doping degree of PEDOT. For the PP-g-PAA/PEDOT composite fibers prepared with $FeCl_3$ as oxidant, fast response time (less than 2 s) and high relative resistance changes (63% for HCl and 110% for NH_3 gas) can be achieved for HCl and NH_3 gas detection. The first sensing cycle for both HCl and NH_3 result in a kind of conditioning of the sensor, and following this conditioning step the further cycles are stable in response behavior. Despite irreversible change in resistance existing in the first cycle, good reversibility in response to both HCl and NH_3 gas are obtained starting from the second cycle. The characteristics of the composite sensing fibers can be marked by easy preparation, rapid response and recovery indicating that they have great potential for applications as flexible sensors in smart textiles.

Acknowledgements

We acknowledge financial support from Natural Science Foundation of China (51273040 and 21274019), Program for Changjiang Scholars and Innovative Research Team in University (T2011079, IRT1221), National Natural Science Foundation for Distinguished Young Scholar of China (50925312), Shanghai Fundamental Research Projects (16JC1400701), and Program of Introducing Talents of Discipline to Universities in China (111-2-04). We thank Prof. Zhongyang Cheng (Auburn University) for proof reading the article.

References

[1] R.A. Steven, A.S. Henry, A review of power harvesting using piezoelectric materials (2003–2006), Smart Mater. Struct. 16 (2007) R1.
[2] L. Sun, W.M. Huang, Z. Ding, Y. Zhao, C.C. Wang, H. Purnawali, C. Tang, Stimulus-responsive shape memory materials: a review, Mater. Des. 33 (2012) 577–640.
[3] M.D. Hager, P. Greil, C. Leyens, S. van der Zwaag, U.S. Schubert, Self-healing materials, Adv. Mater. 22 (2010) 5424–5430.
[4] R.A. Potyrailo, V.M. Mirsky, Combinatorial and high-throughput development of sensing materials: the first 10 years, Chem. Rev. 108 (2008) 770–813.
[5] E. Hür, A. Arslan, D. Hür, Synthesis and electrochemical polymerization of a novel 2-(thiophen-2-yl)-4-(thiophen-2-ylmethylene)oxazol-5(4H)-one monomer for supercapacitor applications, React. Funct. Polym. 99 (2016) 35–41.
[6] S.I. Cho, S.B. Lee, Fast electrochemistry of conductive polymer nanotubes: synthesis, mechanism, and application, Acc. Chem. Res. 41 (2008) 699–707.
[7] H.-J. Shin, S.S. Jeon, S.S. Im, CNT/PEDOT core/shell nanostructures as a counter electrode for dye-sensitized solar cells, Synth. Met. 161 (2011) 1284–1288.
[8] H. Yoon, M. Chang, J. Jang, Formation of 1D poly(3,4-ethylenedioxythiophene) nanomaterials in reverse microemulsions and their application to chemical sensors, Adv. Funct. Mater. 17 (2007) 431–436.
[9] N.B. Clark, L.J. Maher, Non-contact, radio frequency detection of ammonia with a printed polyaniline sensor, React. Funct. Polym. 69 (2009) 594–600.
[10] A.A. Khan, M. Khalid, U. Baig, Synthesis and characterization of polyaniline–titanium(IV)phosphate cation exchange composite: methanol sensor and isothermal stability in terms of DC electrical conductivity, React. Funct. Polym. 70 (2010) 849–855.
[11] L. Ruangchuay, A. Sirivat, J. Schwank, Selective conductivity response of polypyrrole-based sensor on flammable chemicals, React. Funct. Polym. 61 (2004) 11–22.
[12] H. Bai, G.Q. Shi, Gas sensors based on conducting polymers, Sensors-Basel 7 (2007) 267–307.
[13] V. Zardetto, T.M. Brown, A. Reale, A. Di Carlo, Substrates for flexible electronics: a practical investigation on the electrical, film flexibility, optical, temperature, and solvent resistance properties, J. Polym. Sci. Polym. Phys. 49 (2011) 638–648.
[14] J. Hong, Z. Pan, M. Yao, X. Zhang, Preparation and properties of continuously produced conductive UHMWPE/PANI composite yarns based on *in situ* polymerization, Synth. Met. 193 (2014) 117–124.
[15] J. Wang, K. Zhang, L. Zhao, W. Ma, T. Liu, Adsorption and polymerization of aniline on a carboxylic group-modified fibrous substrate, Synth. Met. 188 (2014) 6–12.
[16] X. Yang, S. Shang, L. Li, X.-M. Tao, F. Yan, Vapor phase polymerization of 3,4-ethylenedioxythiophene on flexible substrate and its application on heat generation, Polym. Adv. Technol. 22 (2011) 1049–1055.
[17] M.S. Kim, H.K. Kim, S.W. Byun, S.H. Jeong, Y.K. Hong, J.S. Joo, K.T. Song, J.K. Kim, C.J. Lee, J.Y. Lee, PET fabric/polypyrrole composite with high electrical conductivity for EMI shielding, Synth. Met. 126 (2002) 233–239.
[18] Y. Li, X.Y. Cheng, M.Y. Leung, J. Tsang, X.M. Tao, M.C.W. Yuen, A flexible strain sensor from polypyrrole-coated fabrics, Synth. Met. 155 (2005) 89–94.
[19] J. Liang, Y.H. Ma, F. Wang, W.T. Yang, Flexible, highly transparent, and conductive poly(3,4-ethylenedioxythiophene)-polypropylene composite films of nanofibrillar morphology, Chem. Mater. 22 (2010) 4254–4262.

[20] G.E. Collins, L.J. Buckley, Conductive polymer-coated fabrics for chemical sensing, Synth. Met. 78 (1996) 93–101.
[21] Y. Zhu, J. Li, H. He, M. Wan, L. Jiang, Reversible wettability switching of polyaniline-coated fabric, triggered by ammonia gas, Macromol. Rapid Commun. 28 (2007) 2230–2236.
[22] K.H. Hong, K.W. Oh, T.J. Kang, Polyaniline-nylon 6 composite fabric for ammonia gas sensor, J. Appl. Polym. Sci. 92 (2004) 37–42.
[23] P. Lv, Y. Zhao, F. Liu, G. Li, X. Dai, X. Ji, Z. Dong, X. Qiu, Fabrication of polyaniline/polyimide composite fibers with electrically conductive properties, Appl. Surf. Sci. 367 (2016) 335–341.
[24] Y. Li, X.Y. Cheng, M.Y. Leung, J. Tsang, X.M. Tao, C.W.M. Yuen, A flexible strain sensor from polypyrrole-coated fabrics, Synth. Met. 155 (2005) 89–94.
[25] S. Kirchmeyer, K. Reuter, Scientific importance, properties and growing applications of poly(3,4-ethylenedioxythiophene), J. Mater. Chem. 15 (2005) 2077–2088.
[26] K.H. Hong, K.W. Oh, T.J. Kang, Preparation and properties of electrically conducting textiles by *in situ* polymerization of poly(3,4-ethylenedioxythiophene), J. Appl. Polym. Sci. 97 (2005) 1326–1332.
[27] T. Bashir, M. Skrifvars, N.K. Persson, Synthesis of high performance, conductive PEDOT-coated polyester yarns by OCVD technique, Polym. Adv. Technol. 23 (2012) 611–617.
[28] H. Ma, R.H. Davis, C.N. Bowman, A novel sequential photoinduced living graft polymerization, Macromolecules 33 (1999) 331–335.
[29] A. Elschner, S. Kirchmeyer, W. Lovenich, U. Merker, K. Reuter, PEDOT: Principles and Applications of an Intrinsically Conductive Polymer, CRC Press, New York, 2010 91–92.
[30] Q. Fan, Z. Qin, T. Villmow, J. Pionteck, P. Pötschke, Y. Wu, B. Voit, M. Zhu, Vapor sensing properties of thermoplastic polyurethane multifilament covered with carbon nanotube networks, Sensors Actuators B Chem. 156 (2011) 63–70.
[31] S.Q. Zhu, D.E. Hirt, Improving the wettability of deep-groove polypropylene fibers by photografting, Text. Res. J. 79 (2009) 534–547.
[32] A.V. Janorkar, A.T. Metters, D.E. Hirt, Modification of poly(lactic acid) films: enhanced wettability from surface-confined photografting and increased degradation rate due to an artifact of the photografting process, Macromolecules 37 (2004) 9151–9159.
[33] C. Kvarnström, H. Neugebauer, S. Blomquist, H.J. Ahonen, J. Kankare, A. Ivaska, *In situ* spectroelectrochemical characterization of poly(3,4-ethylenedioxythiophene), Electrochim. Acta 44 (1999) 2739–2750.
[34] J.W. Choi, M.G. Han, S.Y. Kim, S.G. Oh, S.S. Im, Poly(3,4-ethylenedioxythiophene) nanoparticles prepared in aqueous DBSA solutions, Synth. Met. 141 (2004) 293–299.
[35] J. Jang, M. Chang, H. Yoon, Chemical sensors based on highly conductive poly(3,4-ethylenedioxythiophene) nanorods, Adv. Mater. 17 (2005) 1616–1620.